Neutron stars and strange stars in the chiral SU(3) quark mean field model

P. Wang,[1,2] S. Lawley,[1,2] D. B. Leinweber,[1] A. W. Thomas,[2] and A. G. Williams[1]

[1]*Special Research Center for the Subatomic Structure of Matter (CSSM) and Department of Physics, University of Adelaide 5005, Australia*

[2]*Jefferson Laboratory, 12000 Jefferson Ave., Newport News, Virginia 23606 USA*

(Received 6 June 2005; published 27 October 2005)

We investigate the equations of state for pure neutron matter and for nonstrange and strange hadronic matter in β equilibrium, including Λ, Σ, and Ξ hyperons. The masses and radii of these kinds of stars are obtained. For a pure neutron star, the maximum mass is about $1.8M_{\rm sun}$, while for a strange (nonstrange) hadronic star in β equilibrium, the maximum mass is around $1.45M_{\rm sun}$ ($1.7M_{\rm sun}$). The typical radii of pure neutron stars and strange hadronic stars are about 11.5–13.0 km and 11.5–12.5 km, respectively.

DOI: 10.1103/PhysRevC.72.045801 PACS number(s): 26.60.+c, 12.39.−x, 21.65.+f, 21.80.+a

I. INTRODUCTION

Hadronic matter under extreme conditions has attracted a lot of interest in recent years. On the one hand, many theoretical and experimental efforts have been devoted to the discussion of heavy ion collisions at high temperatures. On the other hand, the physics of neutron stars has become a hot topic that connecting astrophysics with high-density nuclear physics. In 1934, Baade and Zwicky [1] suggested that neutron stars could be formed in supernovae. The first theoretical calculation of a neutron star was performed by Oppenheimer and Volkoff [2] and independently by Tolman [3]. Observing a range of masses and radii of neutron stars will reveal the equations of state (EOS) of dense hadronic matter. Determination of the EOS of neutron stars has been an important goal for more than two decades. Six double neutron-star binaries are known so far, and all of them have masses in the surprisingly narrow range of $1.36 \pm 0.08M_{\rm sun}$ [4,5]. A number of early theoretical investigations on neutron stars were based on the nonrelativistic Skyrme framework [6]. Since the Walecka model [7] was proposed and applied to study the properties of nuclear matter, the relativistic mean field approach has been widely used in the determination of the masses and radii of neutron stars. These models lead to different predictions for neutron-star masses and radii [8,9]. For a recent review, see Ref. [10]. Though models with maximum neutron-star masses considerably smaller than $1.4M_{\rm sun}$ are simply ruled out, the constraint on EOS of nuclear matter (for example, the density dependence of pressure of a hadronic system) has certainly not been established from the existing observations.

In the process of neutron-star formation, β equilibrium can be achieved. As a consequence, hyperons will exist in neutron stars, especially in stars with high baryon densities. These hyperons will affect the EOS of hadronic matter. As a result, the mass-radius relationship of strange hadronic stars will be quite different from that of pure neutron stars. The simplest way to discuss the effects of hyperons is to study strange hadronic stars including only Λ hyperons. This is because Λ is the lightest hyperon and the Λ-N interaction is known better than other hyperon-nucleon interactions. However, one must also consider hyperons with negative charge in neutron stars because the negatively charged hyperons can substitute for electrons. There have been many discussions of strange hadronic stars including Λ hyperons, Λ and Σ^-, or even the whole baryon octet [11–20].

At high baryon density, the overlap effects of baryons are very important, and the quark degrees of freedom within baryons should be considered. Some phenomenological models are based on the quark degrees of freedom, such as the quark-meson coupling model [21], the cloudy bag model [22], the quark mean field model [23], and the Nambu-Jona-Lasinio (NJL) model [24]. Several years ago, a chiral SU(3) quark mean field model was proposed [25,26]. In this model, quarks are confined within baryons by an effective potential. The quark-meson interaction and meson self-interaction are based on SU(3) chiral symmetry. Through the mechanism of spontaneous symmetry breaking, the resulting constituent quarks and mesons (except for the pseudoscalars) obtain masses. The introduction of an explicit symmetry breaking term in the meson self-interaction generates the masses of the pseudoscalar mesons which satisfy the partially conserved axial-vector current (PCAC) relations. The explicit symmetry breaking term in the quark-meson interaction gives reasonable hyperon potentials in hadronic matter. This chiral SU(3) quark mean field model has been applied to investigate nuclear matter [27], strange hadronic matter [25], finite nuclei, hypernuclei [26], and quark matter [28]. Recently, we improved the chiral SU(3) quark mean field model by using the linear definition of effective baryon mass [29]. This new treatment is applied to study the liquid-gas phase transition of an asymmetric nuclear system and strange hadronic matter [30,31]. By and large the results are in reasonable agreement with existing experimental data.

In this paper, we will study the neutron star and strange star in the chiral SU(3) quark mean field model. The paper is organized in the following way. In Sec. II, we briefly introduce the model. In Sec. III, we apply this model to investigate the neutron star and strange hadronic star. The numerical results are discussed in Sec. IV. We summarize the main results in Sec. V.

II. THE MODEL

Our considerations are based on the chiral SU(3) quark mean field model (for details see Refs. [25,26]), which contains quarks and mesons as the basic degrees of freedom. In the chiral limit, the quark field Ψ can be split into left- and right-handed parts Ψ_L and Ψ_R: $\Psi = \Psi_L + \Psi_R$. Under $SU(3)_L \times SU(3)_R$ they transform as

$$\Psi_L \to \Psi'_L = L\,\Psi_L, \quad \Psi_R \to \Psi'_R = R\,\Psi_R. \tag{1}$$

The spin-0 mesons are written in the compact form

$$\begin{matrix} M \\ M^\dagger \end{matrix} = \Sigma \pm i\Pi = \frac{1}{\sqrt{2}}\sum_{a=0}^{8}(s^a \pm i p^a)\lambda^a, \tag{2}$$

where s^a and p^a are the nonets of scalar and pseudoscalar mesons, respectively, $\lambda^a (a = 1, \ldots, 8)$ are the Gell-Mann matrices, and $\lambda^0 = \sqrt{\frac{2}{3}}\,I$. The alternatives indicated by the plus and minus signs correspond to M and $M^\dagger$, respectively. Under chiral SU(3) transformations, M and $M^\dagger$ transform as $M \to M' = LMR^\dagger$ and $M^\dagger \to M^{\dagger\prime} = RM^\dagger L^\dagger$. The spin-1 mesons are arranged in a similar way as

$$\begin{matrix} l_\mu \\ r_\mu \end{matrix} = \frac{1}{2}(V_\mu \pm A_\mu) = \frac{1}{2\sqrt{2}}\sum_{a=0}^{8}\left(v_\mu^a \pm a_\mu^a\right)\lambda^a, \tag{3}$$

with the transformation properties $l_\mu \to l'_\mu = L l_\mu L^\dagger$ and $r_\mu \to r'_\mu = R r_\mu R^\dagger$. The matrices Σ, Π, V_μ, and A_μ can be written in a form where the physical states are explicit. For the scalar and vector nonets, we have the expressions

$$\Sigma = \frac{1}{\sqrt{2}}\sum_{a=0}^{8} s^a\lambda^a = \begin{pmatrix} \frac{1}{\sqrt{2}}\left(\sigma + a_0^0\right) & a_0^+ & K^{*+} \\ a_0^- & \frac{1}{\sqrt{2}}\left(\sigma - a_0^0\right) & K^{*0} \\ K^{*-} & \bar{K}^{*0} & \zeta \end{pmatrix}, \tag{4}$$

$$V_\mu = \frac{1}{\sqrt{2}}\sum_{a=0}^{8} v_\mu^a\lambda^a = \begin{pmatrix} \frac{1}{\sqrt{2}}\left(\omega_\mu + \rho_\mu^0\right) & \rho_\mu^+ & K_\mu^{*+} \\ \rho_\mu^- & \frac{1}{\sqrt{2}}\left(\omega_\mu - \rho_\mu^0\right) & K_\mu^{*0} \\ K_\mu^{*-} & \bar{K}_\mu^{*0} & \phi_\mu \end{pmatrix}. \tag{5}$$

Pseudoscalar and pseudovector nonet mesons can be written in a similar fashion.

The total effective Lagrangian is written

$$\mathcal{L}_{\rm eff} = \mathcal{L}_0 + \mathcal{L}_{qM} + \mathcal{L}_{\Sigma\Sigma} + \mathcal{L}_{VV} + \mathcal{L}_{\chi SB} + \mathcal{L}_{\Delta m_s} + \mathcal{L}_h + \mathcal{L}_c, \tag{6}$$

where $\mathcal{L}_0 = i\bar{\Psi}\gamma^\mu\partial_\mu\Psi$ is the free part for massless quarks. The quark-meson interaction $\mathcal{L}_{qM}$ can be written in a chiral SU(3) invariant way as

$$\begin{aligned} \mathcal{L}_{qM} &= g_s(\bar{\Psi}_L M \Psi_R + \bar{\Psi}_R M^\dagger \Psi_L) \\ &\quad - g_v(\bar{\Psi}_L\gamma^\mu l_\mu\Psi_L + \bar{\Psi}_R\gamma^\mu r_\mu\Psi_R) \\ &= \frac{g_s}{\sqrt{2}}\bar{\Psi}\left(\sum_{a=0}^{8} s_a\lambda_a + i\gamma^5\sum_{a=0}^{8} p_a\lambda_a\right)\Psi \\ &\quad - \frac{g_v}{2\sqrt{2}}\bar{\Psi}\left(\gamma^\mu\sum_{a=0}^{8} v_\mu^a\lambda_a - \gamma^\mu\gamma^5\sum_{a=0}^{8} a_\mu^a\lambda_a\right)\Psi. \end{aligned} \tag{7}$$

From the quark-meson interaction, the coupling constants between scalar mesons, vector mesons, and quarks have the following relations:

$$\begin{aligned} &\frac{g_s}{\sqrt{2}} = g_{a_0}^u = -g_{a_0}^d = g_\sigma^u = g_\sigma^d = \cdots = \frac{1}{\sqrt{2}}g_\zeta^s, \\ &g_{a_0}^s = g_\sigma^s = g_\zeta^u = g_\zeta^d = 0, \end{aligned} \tag{8}$$

$$\begin{aligned} &\frac{g_v}{2\sqrt{2}} = g_\rho^u = -g_\rho^d = g_\omega^u = g_\omega^d = \cdots = \frac{1}{\sqrt{2}}g_\phi^s, \\ &g_\omega^s = g_\rho^s = g_\phi^u = g_\phi^d = 0. \end{aligned} \tag{9}$$

In the mean field approximation, the chiral-invariant scalar meson $\mathcal{L}_{\Sigma\Sigma}$ and vector meson $\mathcal{L}_{VV}$ self-interaction terms are written as [25,26]

$$\begin{aligned} \mathcal{L}_{\Sigma\Sigma} &= -\frac{1}{2}k_0\chi^2(\sigma^2 + \zeta^2) + k_1(\sigma^2 + \zeta^2)^2 \\ &\quad + k_2\left(\frac{\sigma^4}{2} + \zeta^4\right) + k_3\chi\sigma^2\zeta \\ &\quad - k_4\chi^4 - \frac{1}{4}\chi^4\ln\frac{\chi^4}{\chi_0^4} + \frac{\delta}{3}\chi^4\ln\frac{\sigma^2\zeta}{\sigma_0^2\zeta_0}, \end{aligned} \tag{10}$$

$$\begin{aligned} \mathcal{L}_{VV} &= \frac{1}{2}\frac{\chi^2}{\chi_0^2}\left(m_\omega^2\omega^2 + m_\rho^2\rho^2 + m_\phi^2\phi^2\right) \\ &\quad + g_4(\omega^4 + 6\omega^2\rho^2 + \rho^4 + 2\phi^4), \end{aligned} \tag{11}$$

where $\delta = 6/33$; σ_0 and ζ_0 are the vacuum expectation values of the corresponding mean fields σ, ζ which are expressed as

$$\sigma_0 = -F_\pi, \quad \zeta_0 = \frac{1}{\sqrt{2}}(F_\pi - 2F_K). \tag{12}$$

The vacuum value χ_0 is about 280 MeV in our numerical calculation. The Lagrangian $\mathcal{L}_{\chi SB}$ generates the nonvanishing masses of pseudoscalar mesons

$$\mathcal{L}_{\chi SB} = \frac{\chi^2}{\chi_0^2}\left[m_\pi^2 F_\pi\sigma + \left(\sqrt{2}m_K^2 F_K - \frac{m_\pi^2}{\sqrt{2}}F_\pi\right)\zeta\right], \tag{13}$$

leading to a nonvanishing divergence of the axial currents which in turn satisfy the PCAC relations for π and K mesons. Pseudoscalar and scalar mesons and also the dilaton field χ obtain mass terms by spontaneous breaking of chiral symmetry in the Lagrangian of Eq. (10). The masses of u, d, and s quarks are generated by the vacuum expectation values of the two scalar mesons σ and ζ. To obtain the correct constituent mass of the strange quark, an additional mass term has to be added:

$$\mathcal{L}_{\Delta m_s} = -\Delta m_s\bar{q}Sq, \tag{14}$$

where $S = \frac{1}{3}(I - \lambda_8\sqrt{3}) = \mathrm{diag}(0, 0, 1)$ is the strangeness quark matrix. Based on these mechanisms, the quark constituent masses are finally given by

$$m_u = m_d = -\frac{g_s}{\sqrt{2}}\sigma_0 \quad \text{and} \quad m_s = -g_s\zeta_0 + \Delta m_s. \tag{15}$$

The parameters $g_s = 4.76$ and $\Delta m_s = 29$ MeV are chosen to yield the constituent quark masses $m_q = 313$ and $m_s = 490$ MeV. The hyperon potential felt by baryon j in i matter is defined as

$$U_j^{(i)} = M_j^* - M_j + g_\omega^j \omega + g_\phi^j \phi. \quad (16)$$

To obtain reasonable hyperon potentials in hadronic matter, we include an additional coupling between strange quarks and the scalar mesons σ and ζ [25]. This term is expressed as

$$\mathcal{L}_h = [h_1(\sigma - \sigma_0) + h_2(\zeta - \zeta_0)]\bar{s}s. \quad (17)$$

Therefore, the strange quark scalar-coupling constants are modified and do not exactly satisfy Eq. (8). In the quark mean field model, quarks are confined in baryons by the Lagrangian $\mathcal{L}_c = -\bar{\Psi}\chi_c\Psi$ [with χ_c given in Eq. (18), below]. We note that this confining term is not chiral invariant. Possible extensions of the model that would restore chiral symmetry in this term have been discussed in Ref. [32].

The Dirac equation for a quark field Ψ_{ij} under the additional influence of the meson mean fields is given by

$$[-i\vec{\alpha}\cdot\vec{\nabla} + \beta\chi_c(r) + \beta m_i^*]\Psi_{ij} = e_i^*\Psi_{ij}, \quad (18)$$

where $\vec{\alpha} = \gamma^0\vec{\gamma}$, $\beta = \gamma^0$, the subscripts i and j denote the quark i ($i = u, d, s$) in a baryon of type j ($j = N, \Lambda, \Sigma, \Xi$) and $\chi_c(r)$ is a confinement potential, i.e., a static potential providing the confinement of quarks by meson mean field configurations. In the numerical calculations, we choose $\chi_c(r) = \frac{1}{4}k_c r^2$, where $k_c = 1$ (GeV fm^{-2}), which yields baryon radii (in the absence of the pion cloud [33]) around 0.6 fm. The quark mass m_i^* and energy e_i^* are defined as

$$m_i^* = -g_\sigma^i\sigma - g_\zeta^i\zeta + m_{i0} \quad (19)$$

and

$$e_i^* = e_i - g_\omega^i\omega - g_\rho^i\rho - g_\phi^i\phi, \quad (20)$$

where e_i is the energy of the quark under the influence of the meson mean fields. Here $m_{i0} = 0$ for $i = u, d$ (nonstrange quark) and $m_{i0} = \Delta m_s$ for $i = s$ (strange quark). The effective baryon mass can be written as

$$M_j^* = \sum_i n_{ij}e_i^* - E_j^0, \quad (21)$$

where n_{ij} is the number of quarks with flavor i in a baryon with flavor j, with $j = N\{p, n\}$, $\Sigma\{\Sigma^\pm, \Sigma^0\}$, $\Xi\{\Xi^0, \Xi^-\}$, and Λ; and E_j^0 is only very weakly dependent on the external field strength. We therefore use Eq. (21), with E_j^0 a constant, independent of the density, which is adjusted to give a best fit to the free baryon masses. Here we use the linear definition of effective baryon mass instead of the earlier square root ansätz. As we explained in Ref. [29], the linear definition of effective baryon mass has been derived using a symmetric relativistic approach [34], while to the best of our knowledge, no equivalent derivation exists for the square root case.

III. HADRONIC SYSTEM

Based on the previously defined quark mean field model, the thermodynamical potential for the study of hadronic systems is written as

$$\Omega = \sum_{j=N,\Lambda,\Sigma,\Xi} \frac{-2k_BT}{(2\pi)^3}\int_0^\infty d^3k\{\ln(1+e^{-(E_j^*(k)-\nu_j)/k_BT}) + \ln(1+e^{-(E_j^*(k)+\nu_j)/k_BT})\} - \mathcal{L}_M, \quad (22)$$

where $E_j^*(k) = \sqrt{M_j^{*2} + k^2}$ and M_j^* is the effective baryon mass. The quantity ν_j is related to the usual chemical potential μ_j by $\nu_j = \mu_j - g_\omega^j\omega - g_\rho^j\rho - g_\phi^j\phi$. The mesonic Lagrangian

$$\mathcal{L}_M = \mathcal{L}_{\Sigma\Sigma} + \mathcal{L}_{VV} + \mathcal{L}_{\chi SB} \quad (23)$$

describes the interaction between mesons, which includes the scalar meson self-interaction $\mathcal{L}_{\Sigma\Sigma}$, the vector meson self-interaction $\mathcal{L}_{VV}$, and the explicit chiral symmetry-breaking term $\mathcal{L}_{\chi SB}$ defined previously in Eqs. (10), (11), and (13). The Lagrangian $\mathcal{L}_M$ involves scalar (σ, ζ, and χ) and vector (ω, ρ, and ϕ) mesons. The interactions between quarks and scalar mesons result in the effective baryon masses M_j^*. The interactions between quarks and vector mesons generate the baryon-vector meson interaction terms. The energy per volume and the pressure of the system can be derived as $\varepsilon = \Omega - \frac{1}{T}\frac{\partial\Omega}{\partial T} + \nu_j\rho_j$ and $p = -\Omega$, where ρ_j is the density of baryon j. At zero temperature, Ω can be expressed as

$$\Omega = -\sum_{j=N,\Lambda,\Sigma,\Xi}\frac{1}{24\pi^2}\left\{\nu_j\left[\nu_j^2 - M_j^{*2}\right]^{1/2}\left[2\nu_j^2 - 5M_j^{*2}\right] + 3M_j^{*4}\ln\left[\frac{\nu_j + \left(\nu_j^2 - M_j^{*2}\right)^{1/2}}{M_j^*}\right]\right\} - \mathcal{L}_M. \quad (24)$$

The equations for mesons ϕ_i can be obtained by the formula $\frac{\partial\Omega}{\partial\phi_i} = 0$. Therefore, the equations for σ, ζ, and χ are

$$k_0\chi^2\sigma - 4k_1(\sigma^2+\zeta^2)\sigma - 2k_2\sigma^3 - 2k_3\chi\sigma\zeta - \frac{2\delta}{3\sigma}\chi^4 + \frac{\chi^2}{\chi_0^2}m_\pi^2F_\pi - \left(\frac{\chi}{\chi_0}\right)^2 m_\omega\omega^2\frac{\partial m_\omega}{\partial\sigma} - \left(\frac{\chi}{\chi_0}\right)^2 m_\rho\rho^2\frac{\partial m_\rho}{\partial\sigma} + \sum_{j=N,\Lambda,\Sigma,\Xi}\frac{\partial M_j^*}{\partial\sigma}\langle\bar{\psi}_j\psi_j\rangle = 0, \quad (25)$$

$$k_0\chi^2\zeta - 4k_1(\sigma^2+\zeta^2)\zeta - 4k_2\zeta^3 - k_3\chi\sigma^2 - \frac{\delta}{3\zeta}\chi^4 + \frac{\chi^2}{\chi_0^2}\left(\sqrt{2}m_k^2F_k - \frac{1}{\sqrt{2}}m_\pi^2F_\pi\right) - \left(\frac{\chi}{\chi_0}\right)^2 m_\phi\phi^2\frac{\partial m_\phi}{\partial\zeta} + \sum_{j=\Lambda,\Sigma,\Xi}\frac{\partial M_j^*}{\partial\zeta}\langle\bar{\psi}_j\psi_j\rangle = 0, \quad (26)$$

$$k_0\chi(\sigma^2+\zeta^2) - k_3\sigma^2\zeta + \left(4k_4 + 1 + 4\ln\frac{\chi}{\chi_0} - \frac{4\delta}{3}\ln\frac{\sigma^2\zeta}{\sigma_0^2\zeta_0}\right)\chi^3 + \frac{2\chi}{\chi_0^2}\left[m_\pi^2F_\pi\sigma + \left(\sqrt{2}m_k^2F_k - \frac{1}{\sqrt{2}}m_\pi^2F_\pi\right)\zeta\right] - \frac{\chi}{\chi_0^2}\left(m_\omega^2\omega^2 + m_\rho^2\rho^2 + m_\phi^2\phi^2\right) = 0, \quad (27)$$

TABLE I. Hyperon potentials in MeV.

$U_N^{(N)}$	$U_\Lambda^{(N)}$	$U_\Sigma^{(N)}$	$U_\Xi^{(N)}$	$U_\Lambda^{(\Lambda)}$	$U_\Sigma^{(\Lambda)}$	$U_\Xi^{(\Lambda)}$	$U_\Lambda^{(\Xi)}$	$U_\Sigma^{(\Xi)}$	$U_\Xi^{(\Xi)}$
−64.0	−28.0	−28.0	8.0	−24.5	−24.5	−20.6	−30.6	−30.6	−50.3

where $\langle\bar{\psi}_j\psi_j\rangle$ is expressed as

$$\langle\bar{\psi}_j\psi_j\rangle = \frac{M_j^*}{\pi^2}\int_0^{k_{F_j}} dk \frac{k^2}{\sqrt{M_j^{*2}+k^2}} = \frac{M_j^{*3}}{2\pi^2}\left[\frac{k_{F_j}}{M_j^*}\sqrt{1+\frac{k_{F_j}^2}{M_j^{*2}}} - \ln\left(\frac{k_{F_j}}{M_j^*}+\sqrt{1+\frac{k_{F_j}^2}{M_j^{*2}}}\right)\right], \quad (28)$$

with $k_{F_j} = \sqrt{\nu_j^2 - M_j^{*2}}$.

For the β equilibrium, the chemical potentials for the baryons satisfy the following equations:

$$\mu_\Lambda = \mu_{\Sigma^0} = \mu_{\Xi^0} = \mu_n = \mu_p + \mu_e = \mu_p + \mu_\mu, \quad (29)$$

$$\mu_{\Sigma^+} = \mu_p, \quad (30)$$

$$\mu_{\Sigma^-} = \mu_{\Xi^-} = \mu_n + \mu_e. \quad (31)$$

There are only two independent chemical potentials which are determined by the total baryon density and neutral charge:

$$\rho_B = \rho_p + \rho_n + \rho_\Lambda + \rho_{\Sigma^+} + \rho_{\Sigma^0} + \rho_{\Sigma^-} + \rho_{\Xi^0} + \rho_{\Xi^-}, \quad (32)$$

$$\rho_p + \rho_{\Sigma^+} - \rho_{\Sigma^-} - \rho_{\Xi^-} - \rho_e - \rho_\mu = 0. \quad (33)$$

To get the mass-radius relation, one has to resolve the Tolman-Oppenheimer-Volkoff (TOV) equation:

$$\frac{dp}{dr} = -\frac{[p(r)+\varepsilon(r)][M(r)+4\pi r^3 p(r)]}{r(r-2M(r))}, \quad (34)$$

where

$$M(r) = 4\pi\int_0^r \varepsilon(r)r^2 dr. \quad (35)$$

With the equations of state, functions such as $M(r)$, $\rho(r)$, $p(r)$, can be obtained.

IV. NUMERICAL RESULTS

The parameters of this model were determined by the meson masses in vacuum and the saturation properties of nuclear matter. The improved linear definition of effective baryon mass is chosen in our numerical calculations. The binding energy of symmetric nuclear matter is 16 MeV, and the saturation density ρ_0 is 0.16 fm^{-3}. The incompression modulus at ρ_0 is 303 MeV. The hyperon potentials are listed in Table I. For the Λ hyperon, the empirical value of $U_\Lambda^{(N)}$ is −28 MeV at the saturation density of nuclear matter ρ_0 [35]. For $U_\Xi^{(N)}$, recent experiments suggest that $U_\Xi^{(N)}$ may be −14 or less [36]. In Λ matter, the typical values of $U_j^{(\Lambda)}$ ($j = \Lambda, \Xi$) are around −20 MeV at density $\rho = \rho_0/2$ [37]. In Ξ matter, $U_j^{(\Xi)}$ ($j = \Lambda, \Xi$) are around −40 MeV at density $\rho = \rho_0$ [37]. From Table I, one can see that though only two parameters h_1 and h_2 are adjusted in this model, most of the hyperon potentials are reasonable.

We first discuss the equations of state of neutron matter and strange hadronic matter which are needed for the calculation of neutron stars. For pure neutron stars, only neutrons are present. For strange hadronic stars, with increasing baryon density, other kinds of baryons will appear. In Fig. 1, we show the fractions of octet baryons versus density with β equilibrium. With increasing baryon density, the neutron fraction decreases slowly from 1. If the density is lower than about 0.19 fm^{-3}, the fraction of electrons is the same as that of protons, which makes the system charge neutral. The muon appears when the density is in the range 0.19–0.98 fm^{-3}. The maximum fractions of muons and electrons appear at $\rho_B \simeq 0.4$ fm^{-3}. Their fractions decrease with increasing fractions of hyperons. When the density is larger than about 0.4 fm^{-3}, the Σ^- hyperons appear and the fraction of neutrons decreases faster. After the density is larger than about 0.57 fm^{-3}, Λ hyperons start to appear. The fraction of Σ^- hyperons decreases with increasing density after Ξ^- hyperons appear where the density is about 0.84 fm^{-3}.

The density dependence of the effective baryon masses and scalar mean fields are shown in Fig. 2. The σ field decreases quickly with the increasing baryon density when the density is small, $\rho_B < 0.4$ fm^{-3}. This is because at small baryon density, the nucleon is dominant and there are no hyperons. With increasing density, more and more hyperons appear. As a result, the ζ field decreases quickly. At a broad range of densities, the value of χ changes little.

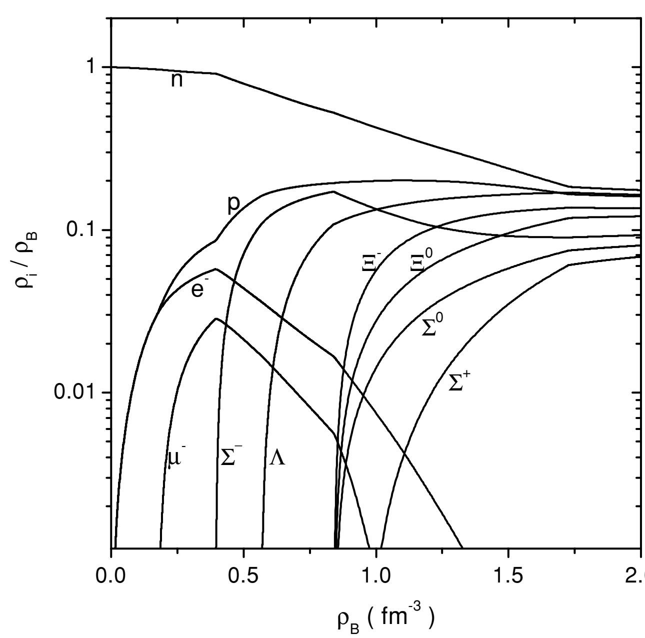

FIG. 1. Fractions of proton, neutron, Λ, Σ, and Ξ of strange hadronic stars vs baryon density with β equilibrium.

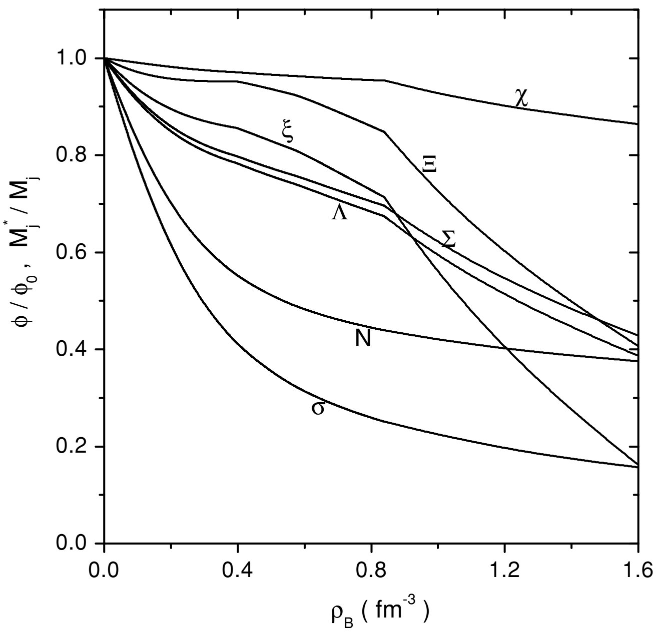

FIG. 2. Effective baryon masses and meson mean fields vs baryon density with β equilibrium.

In Fig. 3, the pressure versus baryon density is shown. When the density is low, the three curves are close to each other. With increasing baryon density, the contribution from protons and hyperons is not negligible. For nuclear matter, some of the protons and neutrons are in states of high energy and momentum when the density is high, because of the Pauli exclusion principle. For strange hadronic matter, nucleons can be replaced by hyperons that are in states with lower kinetic

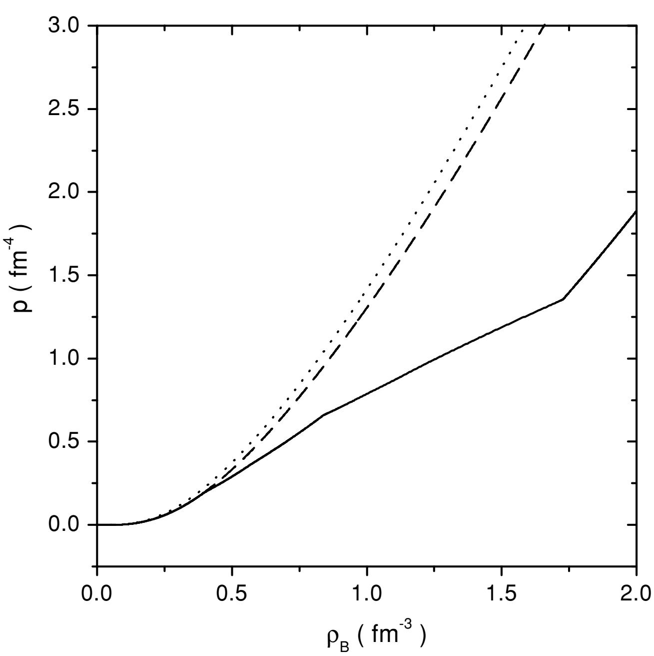

FIG. 3. Pressure of hadronic matter p vs baryon density ρ_B. Dotted, dashed, and solid curves are for pure neutron stars, and for nonstrange and strange hadronic stars with β equilibrium, respectively.

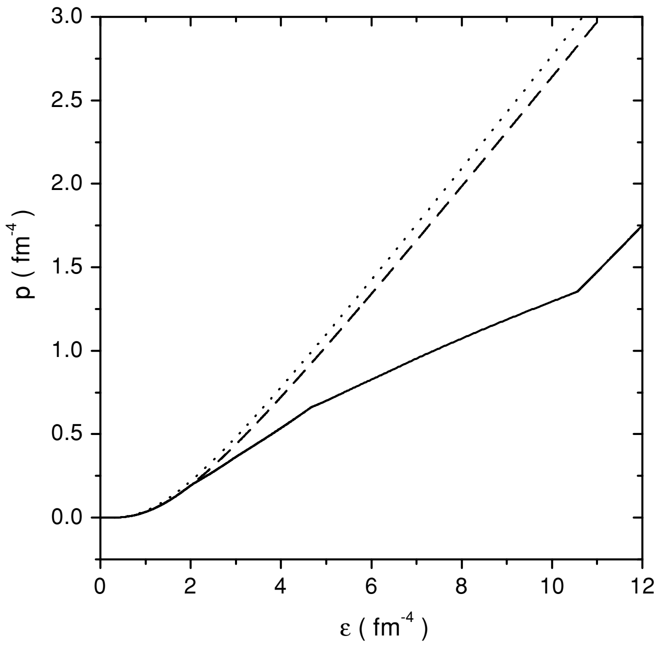

FIG. 4. Pressure of hadronic matter p vs energy density ε. Curves are the same as in Fig. 3.

energy. Thus the momenta of the hyperons are lower, and for a given baryon density, the strange hadronic matter has lower pressure and hence a "softer" equation of state. As plotted in Fig. 3, at a given baryon density, the pressure of strange hadronic matter is the smallest one among these three curves. The pressure p versus energy density ε is shown in Fig. 4. Again, one can see that the equation of state of strange hadronic matter is softer than those in the other two cases.

In Fig. 5, we plot the derivative of pressure with respect to energy per unit volume. At low density, for example, less

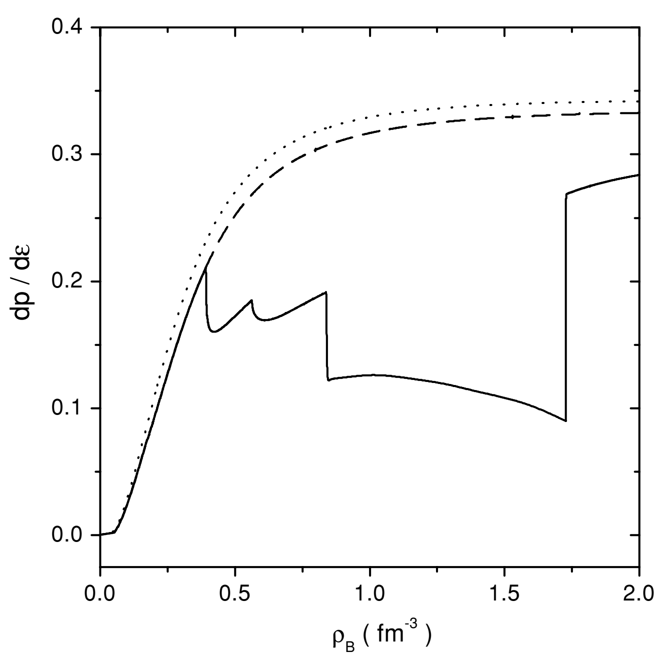

FIG. 5. Derivative of pressure with respect to energy density vs baryon density. Curves are the same as in Fig. 3.

than $2\rho_0$, $dp/d\varepsilon$ is smaller than 0.2. For nonstrange matter, when the baryon density is larger than about $4\rho_0$, $dp/d\varepsilon$ approaches 1/3, which means that the baryons are relativistic. For strange hadronic matter, when hyperons appear, $dp/d\varepsilon$ becomes smaller compared with the other two curves. The nonsmooth change of the curve can be understood from Fig. 4, where the slope of the curve for strange hadronic matter changes discontinuously. This behavior is due to the effect of hyperons (see Fig. 1). Our results are comparable with Ref. [38], where strange hadronic matter was studied in a relativistic mean field model. For strange matter, though the total baryon density can be as large as $10\rho_0$, the density of each kind of baryon is not high enough to make the baryons behave as highly relativistic particles.

We now study neutron stars with the obtained EOS. Because the nucleon crust makes an important contribution to a star's radius, especially for stars with low central density [18,39], we will replace the obtained EOS at low density by those for the crust. At low density, the EOS of Negele and Vautherin [40] are close to those of Baym *et al.* [41]. In the numerical calculation, the crust data in Ref. [40] at density smaller than 0.1 fm^{-3} are used. By solving the TOV equation, the baryon density vs radius can be obtained as shown in Fig. 6. The central densities ρ_c are chosen to be $3\rho_0$ and $5\rho_0$ where ρ_0 (0.16 fm^{-3}) is the saturation density of symmetric nuclear matter. With increasing radius, the density of strange hadronic stars decreases a little faster than that of pure neutron stars, which results in a smaller radius. The radii of stars are not very sensitive to their central density ρ_c when ρ_c is in some region. For example, from the figure, one can see that for $\rho_c = 3\rho_0$ and $\rho_c = 5\rho_0$, the difference of the star radii is less than 1 km. Figure 6 also shows that when the density is lower than about 0.1 fm^{-3}, a nucleon crust exists on the surface of a star with a radius of about several hundred meters. Calculations show that

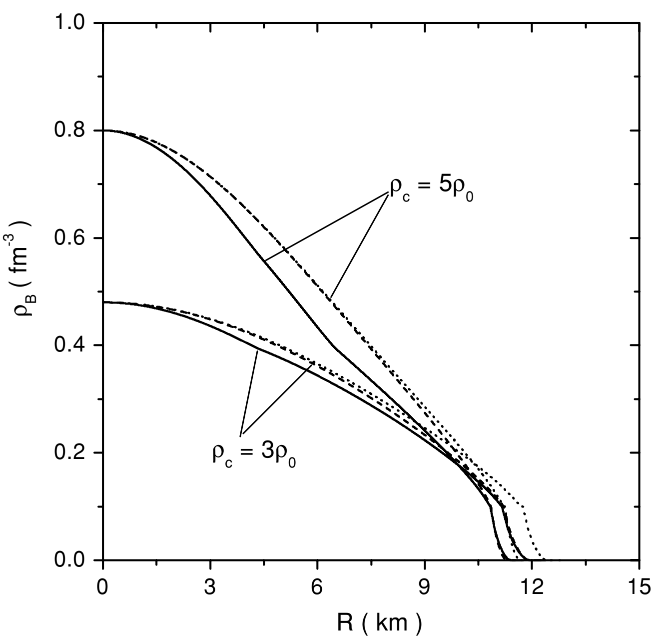

FIG. 6. Baryon density of hadronic stars vs radii. Curves are the same as in Fig. 3.

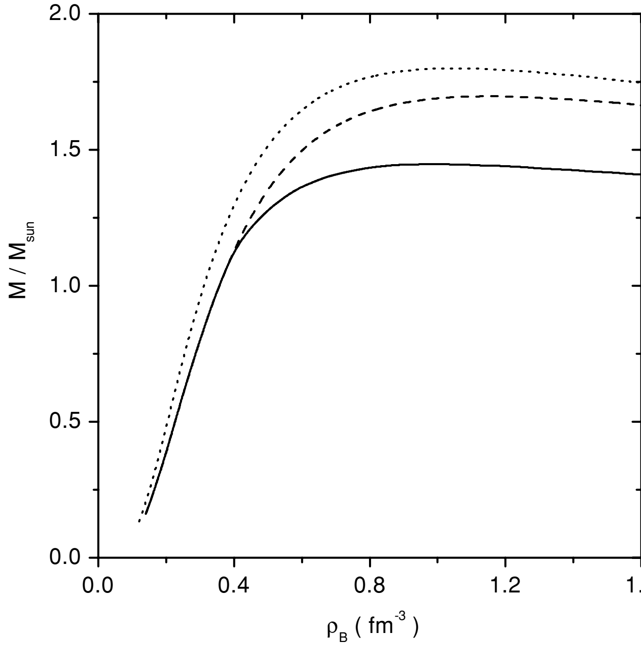

FIG. 7. Masses of hadronic stars vs their central baryon densities. Curves are the same as in Fig. 3.

the nucleon crust has little effect on the star's mass. However, the radius of a neutron star will be increased by the crust contribution, especially in the case of stars with low central density.

We plot the star mass ratio $M/M_{\rm sun}$ versus central baryon density in Fig. 7. The maximum mass of pure neutron stars is about $1.8M_{\rm sun}$ with a central density 1.05 fm^{-3}. Beyond that density, the star becomes unstable. The maximum mass changes to $1.7M_{\rm sun}$ and $1.45M_{\rm sun}$ when proton and hyperons are included. When the central density is smaller than 0.4 fm^{-3}, there is no hyperon. Therefore, the solid and dashed lines are the same in the small density region. In the range $3\rho_0 < \rho_c < 6\rho_0$, the masses of pure neutron stars, and of nonstrange and strange hadronic stars with β equilibrium are $1.48M_{\rm sun} < M < 1.8M_{\rm sun}$, $1.32M_{\rm sun} < M < 1.7M_{\rm sun}$, and $1.25M_{\rm sun} < M < 1.45M_{\rm sun}$, respectively. Our results are reasonable when compared with the observation of the six known stars with masses in the range $1.36 \pm 0.08M_{\rm sun}$, since the "neutron star" is in fact a strange hadronic star with β equilibrium. We should also keep in mind that some heavy stars has been reported in recent years. For PSR J0437-4715, the mass has been found to be $1.58 \pm 0.18M_{\rm sun}$ [42]. For Vale X-1, Cygnus X-2, and 4U 1820-30, their masses have been determined to be $1.87^{+0.23}_{-0.17}M_{\rm sun}$ [43], $1.8 \pm 0.4M_{\rm sun}$ [44], and $\simeq 2.3M_{\rm sun}$ [45,46]. The rotation of a star can increase its mass by $\sim 10\%$ [47]. Therefore, the calculated maximum mass of strange hadronic stars can be as large as $1.6M_{\rm sun}$. If the heavy stars such as 4U 1820-30 are confirmed, the strange hadronic star would be ruled out if this model is a good description of Nature. It is possible to increase the maximum star mass by making the EOS stiffer at higher densities. Whether the inclusion of a quark core in the strange star will result in a large maximum mass is an interesting topic.

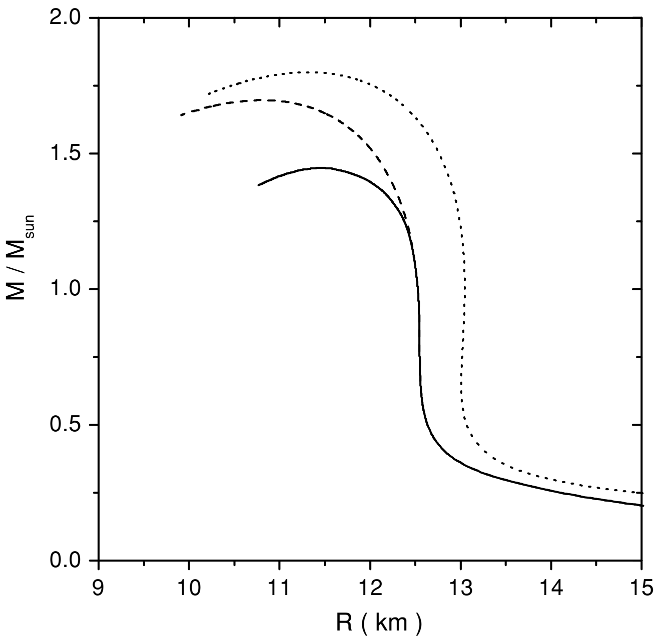

FIG. 8. Masses of hadronic stars vs their radii. Curves are the same as in Fig. 3.

In Fig. 8, the masses of stars versus their radii are shown. For pure neutron stars, when their masses are in the range $0.5M_{\rm sun} < M < 1.8M_{\rm sun}$, their radii are about 11.5–13.0 km. For strange hadronic stars with masses of $0.5M_{\rm sun} < M < 1.45M_{\rm sun}$, the radii are about 11.5–12.5 km. Pure neutron stars have larger radii compared with the stars in β equilibrium. When the star masses are large than about $1.25M_{\rm sun}$, the radii of strange stars are smaller than those of nonstrange stars. Because the size of neutron stars is small, it is very difficult to observe and measure their radii directly. Different indirect methods lead to different values of radii with large errors. For example, for the RX J1856-3754, the radius varies from 5 to 15 km with a mass of $1.4M_{\rm sun}$ [5]. More accurate values are needed to obtain a more strict constraint on the EOS of hadronic matter.

V. SUMMARY

We have investigated neutron stars and strange hadronic stars in the chiral SU(3) quark mean field model. The Λ, Σ, and Ξ hyperons are included in the model. The proton and hyperon contributions to the system are important at high baryon density when β equilibrium is achieved, and they soften the EOS of hadronic matter. The maximum pure neutron star mass is about $M = 1.8M_{\rm sun}$ with a corresponding radius $R = 11.5$ km and central density $\rho_c = 1.05\ {\rm fm}^{-3}$. For strange hadronic stars, the maximum masses are about $1.45M_{\rm sun}$ and the corresponding radii and central density are $R = 11.5$ km and $\rho_c = 1.0\ {\rm fm}^{-3}$. When the central densities are between $3\rho_0$ and $6\rho_0$, the masses of stars are in the ranges $1.25M_{\rm sun} < M < 1.45M_{\rm sun}$ (strange hadronic stars), $1.32M_{\rm sun} < M < 1.7M_{\rm sun}$ (proton-neutron stars with β equilibrium), and $1.48M_{\rm sun} < M < 1.8M_{\rm sun}$ (pure neutron stars). If the masses of stars are larger than $0.5M_{\rm sun}$, the typical values of radii are 11.5–12.5 km (strange hadronic stars), 11.0–12.5 km (proton-neutron stars with β equilibrium), and 11.5–13.0 km (pure neutron stars), respectively. The nucleon crust has little effect on the mass of a star. However, it increases the radius of a star by 0.5–1 km when the star's mass is larger than about $1M_{\rm sun}$.

Our results are reasonable compared with astrophysical observations, where the six known neutron stars have masses in the narrow range $1.36 \pm 0.08M_{\rm sun}$. Accurate values of radii for neutron stars are needed to get a more strict constraint on the EOS of hadronic matter. As for the heavy stars, for example, 4U 1820-30, if its mass $M \simeq 2.3M_{\rm sun}$ is confirmed, then strange hadronic stars are obviously ruled out if the model explored herein is a good description of Nature. It is therefore of interest to see whether including quark degrees of freedom can lead to this large mass.

ACKNOWLEDGMENTS

P.W. thanks the Theory Group at Jefferson Lab for its kind hospitality. This work was supported by the Australian Research Council and by the U.S. Department of Energy Contract DE-AC05-84ER40150, under which SURA operates Jefferson Laboratory.

[1] W. Baade and F. Zwicky, Proc. Nat. Acad. Sci. USA **20**, 255 (1934).
[2] J. R. Oppenheimer and G. M. Volkoff, Phys. Rev. **55**, 374 (1939).
[3] R. C. Tolman, Phys. Rev. **55**, 364 (1939).
[4] S. E. Thorsett and D. Chakrabarty, Astrophys. J. **512**, 288 (1999).
[5] H. Heiselberg, astro-ph/0201465.
[6] P. Bonche, E. Chabanat, P. Haensel, J. Meyer, and R. Schaeffer, Nucl. Phys. **A643**, 441 (1998).
[7] B. D. Serot and J. D. Walecka, Adv. Nucl. Phys. **16**, 1 (1986).
[8] S. F. Ban, J. Li, S. Q. Zhang, H. Y. Jia, J. P. Sang, and J. Meng, Phys. Rev. C **69**, 045805 (2004).
[9] S. Lawley, W. Bentz, and A. W. Thomas, Nucl. Phys. Proc. Suppl. **141**, 29 (2005).
[10] F. Weber, Prog. Part. Nucl. Phys. **04**, 193 (2005).
[11] S. Nishizaki, Y. Yamamoto, and T. Takatsuka, Prog. Theor. Phys. **105**, 607 (2001).
[12] N. K. Glendenning, Phys. Lett. **B114**, 392 (1982); Nucl. Phys. **A493**, 521 (1989).
[13] F. Weber and M. K. Weigel, Nucl. Phys. **A505**, 779 (1989).
[14] Y. Sugahara and H. Toki, Prog. Theor. Phys. **92**, 803 (1994).
[15] J. Schaffner and I. N. Mishustin, Phys. Rev. C **53**, 1416 (1996).
[16] S. Pal, M. Hanauske, I. Zakout, H. Stöcker, and W. Greiner, Phys. Rev. C **60**, 015802 (1999).
[17] S. Balberg and A. Gal, Nucl. Phys. **A265**, 435 (1997).
[18] M. Baldo, G. F. Burgio, and H. -J. Schulze, Phys. Rev. C **58**, 3688 (1998); **61**, 055801 (2000); astro-ph/0312446, talk given at the NATO Advanced Research Workshop on Superdense QCD Matter and Compact Stars, 27 Sep.–4 Oct. 2003, Yerevan, Armenia.
[19] I. Vidana, A. Polls, A. Ramos, L. Engvik, and M. Hjorth-Jensen, Phys. Rev. C **62** 035801 (2000).

[20] T. Maruyama, T. Muto, T. Tatsumi, K. Tsushima, and A. W. Thomas, nucl-th/0502079.
[21] P. A. M. Guichon, Phys. Lett. **B200**, 235 (1988); S. Fleck, W. Bentz, K. Shimizu, and K. Yazaki, Nucl. Phys. **A510**, 731 (1990); K. Saito and A. W. Thomas, Phys. Lett. **B327**, 9 (1994); P. G. Blunden and G. A. Miller, Phys. Rev. C **54**, 359 (1996); H. Müller and B. K. Jennings, Nucl. Phys. **A640**, 55 (1998).
[22] A. W. Thomas, S. Theberge, and G. A. Miller, Phys. Rev. D **24**, 216 (1981); A. W. Thomas, Adv. Nucl. Phys. **13**, 1 (1984); G. A. Miller, A. W. Thomas, and S. Theberge, Phys. Lett. **B91**, 192 (1980).
[23] H. Toki, U. Meyer, A. Faessler, and R. Brockmann, Phys. Rev. C **58**, 3749 (1998).
[24] W. Bentz and A. W. Thomas, Nucl. Phys. **A696**, 138 (2001); M. Buballa, Phys. Rep. **407**, 205 (2005).
[25] P. Wang, Z. Y. Zhang, Y. W. Yu, R. K. Su, and H. Q. Song, Nucl. Phys. **A688**, 791 (2001).
[26] P. Wang, H. Guo, Z. Y. Zhang, Y. W. Yu, R. K. Su, and H. Q. Song, Nucl. Phys. **A705**, 455 (2002).
[27] P. Wang, Z. Y. Zhang, and Y. W. Yu, Commun. Theor. Phys. **36**, 71 (2001).
[28] P. Wang, V. E. Lyubovitskij, Th. Gutsche, and Amand Faessler, Phys. Rev. C **67**, 015210 (2003).
[29] P. Wang, D. B. Leinweber, A. W. Thomas, and A. G. Williams, Nucl. Phys. **A744**, 273 (2004).
[30] P. Wang, D. B. Leinweber, A. W. Thomas, and A. G. Williams, Phys. Rev. C **70**, 055204 (2004).
[31] P. Wang, D. B. Leinweber, A. W. Thomas, and A. G. Williams, Nucl. Phys. **A748**, 226 (2005).
[32] V. E. Lyubovitskij, T. Gutsche, A. Faessler, and E. G. Drukarev, Phys. Rev. D **63**, 054026 (2001); A. W. Thomas, J. Phys. G **7**, L283 (1981).
[33] E. J. Hackett-Jones, D. B. Leinweber, and A. W. Thomas, Phys. Lett. **B494**, 89 (2000).
[34] P. A. M. Guichon, K. Saito, E. Rodionov, and A. W. Thomas, Nucl. Phys. **A601**, 349 (1996).
[35] D. J. Millener, C. B. Dover, and A. Gal, Phys. Rev. C **38**, 2700 (1988).
[36] P. Khaustov *et al.*, Phys. Rev. C **61**, 054603 (2000).
[37] J. Schaffner, C. B. Dover, A. Gal, C. Greiner, D. J. Millener, and H. Stöcher, Ann. Phys. (NY) **235**, 35 (1994).
[38] J. Schaffner-Bielich and A. Gal, Phys. Rev. C **62**, 034311 (2000).
[39] J. M. Lattimer and M. Prakash, Astrophys. J. **550**, 426 (2001).
[40] J. W. Negele and D. Vautherin, Nucl. Phys. **A207**, 298 (1974).
[41] G. Baym, C. Pethick, and Peter Sutherland, Astrophys. J. **170**, 299 (1971); G. Baym, H. A. Bethe, and C. Pethick, Nucl. Phys. **A175**, 225 (1971).
[42] W. van Straten, M. Bailes, M. C. Britton, S. R. Kulkarni, and J. Sarkissian, Nature **412**, 158 (2001).
[43] O. Barziv, L. Kaper, M. H. van Kerkwijk, J. H. Telting, and J. van Paradijs, Astron. Astrophys. astro-ph/0108237; M. H. van Kerkwijk, in *Proceedings of the ESO Workshop on Black Holes in Binaries and Galactic Nuclei, Garching Sept. 1999*, edited by L. Kaper, E. P. J. van den Heuvel, and P. A. Woudt (Springer, Heidelberg, Germany), p. 39.
[44] J. A. Orosz and E. Kuulkers, Mon. Not. R. Astron. Soc. **305**, 1320 (1999).
[45] W. Zhang, T. E. Strohmayer, and J. H. Swank, Astrophys. J. **482**, L167 (1997).
[46] M. C. Miller, F. K. Lamb, and D. Psaltis, Astrophys. J. **508**, 791 (1998).
[47] N. K. Glendenning, *Compact Stars* (Springer, New York, 2000), p. 297.